Draining of the Sea of Chaos: Role of Resonant Transmission and Reflection in an Array of Billiards

R. Brunner, R. Meisels, and F. Kuchar
Institute of Physics, University of Leoben, A-8700 Leoben, Austria

R. Akis and D. K. Ferry
Department of Electrical Engineering and Center for Solid State Electronics Research, Arizona State University, Tempe, Arizona 85287, USA

J. P. Bird
Department of Electrical Engineering, University at Buffalo, Buffalo, New York 14260, USA
(Received 15 November 2006; published 17 May 2007)

We investigate the dynamics of a system of coupled electron billiards by using a magnetic field to dramatically modify the underlying mixed phase space. At specific values of the magnetic field the sea of chaos is drained. At these fields there exist reflected or transmitted orbits associated with maxima and minima in the experimentally observed magnetoresistance. These effects are studied by comparing the classical and quantum-mechanical phase-space dynamics leading to a basic understanding of the role of chaos in the transport in an array of billiards.

DOI: 10.1103/PhysRevLett.98.204101 PACS numbers: 05.45.Mt, 73.63.Kv, 75.47.Jn

The manner in which the quantum states of a system evolve into their classical counterparts has been of interest since the advent of quantum theory [1] and has led to the development of the field of quantum chaos [2,3]. A special place in this field is occupied by the control of chaos [4], by exploiting the specific features of the phase space. While dynamical systems may be purely chaotic or regular, the most ubiquitous in nature are those whose phase space is instead *mixed* [5]. A theory describing a system under nonlinear perturbation is based on the Kolmogorov-Arnold-Moser (KAM) theorem [6]. It states that for small and smooth perturbation and quasiperiodic motions there exists an invariant torus in phase space [3,6]. Violating either of these conditions may induce a change from a KAM to a non-KAM system, with a drastic evolution in the chaotic dynamics. In driven systems, non-KAM behavior has been found under resonant driving conditions [7–10].

The study of quantum chaos in open systems is important, also, to the decoherence theory [11]. This connects the properties of open quantum systems to the existence of a set of *pointer states*, which remain robust in the presence of the environmental coupling, eventually correlating with regular classical orbits (the states within the KAM islands) [11]. The evidence of such pointer states has been provided in the studies of single open quantum dots [12–14]. However, there remain important questions about the one-to-one connection between the classical and quantum descriptions in this problem and its relation to an experimentally observed quantity—the magnetoresistance (MR).

In a classically regular system with 2 degrees of freedom, the periodic and quasiperiodic orbits lie on two-dimensional (2D) invariant tori, constructed from appropriate action-angle variables [15]. If some of these tori are destroyed by a perturbation, chaos will be caused, resulting in a mixed phase space. The action-angle variables of such a system can be associated with two hybrid frequencies (ω_+ and ω_-, see further below). When these frequencies are irrational multiples of one another, a trajectory follows a quasiperiodic KAM orbit [15], without ever repeating itself. Its torus is therefore filled densely by each of its trajectories individually [6]. When ω_+/ω_- is an integer, the trajectories will repeat themselves and periodic orbits are obtained. In such nondriven systems, like the billiards investigated here, ''resonance'' is defined by this condition [2]. Now, the torus is not densely filled by an individual trajectory and in this sense we speak of a non-KAM system.

In this Letter, we show a magnetic field (B) may be used to drive a sequence of transitions between KAM and non-KAM dynamics in an experimentally realizable system, an array of coupled electron billiards (an open quantum-dot array). These systems are defined in a two-dimensional electron gas (2DEG), resulting in 2 degrees of freedom of electron motion. We show the hybrid frequencies of this system may be tuned by a magnetic field, giving features in the low-temperature MR that are directly related to the transitions between KAM and non-KAM dynamics.

The split-gate quantum-dot arrays we study are realized in the 2DEG of a GaAs/AlGaAs heterostructure. Their MR has been measured at cryostat temperatures of 10 mK. The 2DEG areal density, mobility, and mean free path λ are 2.38×10^{15} m^{-2}, 124 m^2/V s, and 10 μm, respectively [16]. λ is much larger than the dot size (≈ 0.4 μm). The actual dot size differs from the lithographic size [Fig. 1(a)] due to fringing fields. From these parameters we also compute a Fermi energy (E_F) of 8.5 meV and a Fermi ve-

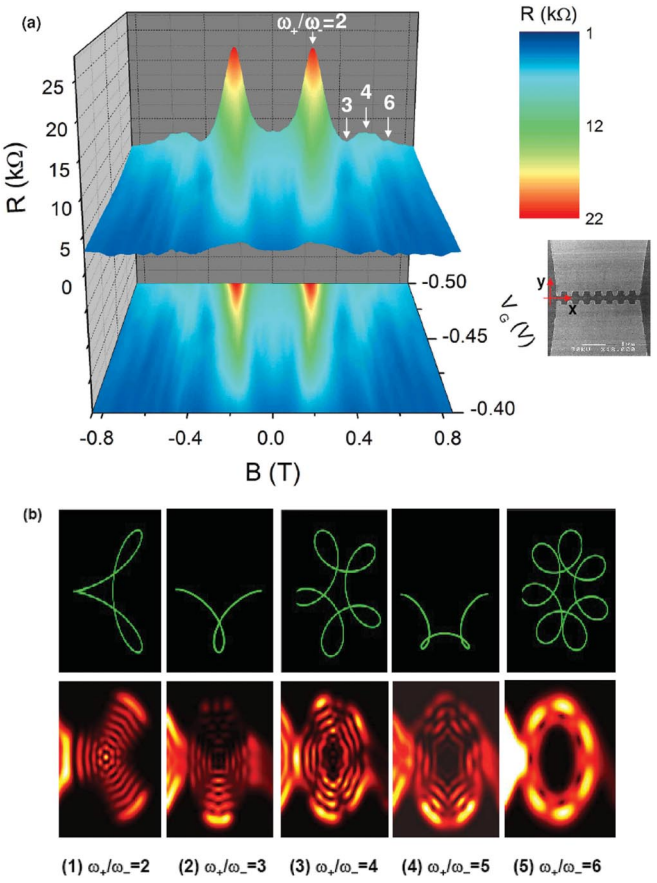

FIG. 1 (color online). (a) Measured MR for the 7-dot array ($T = 10$ mK). Arrows: positions of the resonant maxima and minima expressed by the values of ω_+/ω_-. Inset shows a micrograph of the 7-dot array. (b) Upper row: classically calculated trajectories for certain initial conditions in the entrance constriction. Lower row: QM density probabilities (yellow: highest, black: lowest probability). According to the actual dot shape we chose $\omega_{x,d} = 1.06 \times 10^{12}$ s^{-1}, $\omega_y = 0.85 \times 10^{12}$ s^{-1}, $\omega_{x,c} = 2.16 \times 10^{12}$ s^{-1}; extension in x direction: 0.32 μm (dot region), 0.076 μm (constriction region).

locity (v_F) of 2.1×10^5 m/s. In Ref. [16], the 7-dot array of Fig. 1(a) was studied and, as we show in Fig. 1(a), its MR was found to exhibit a large pair of peaks near ± 0.2 T, with subsidiary peaks near ± 0.5 and ± 0.7 T. As we make clear here, these peaks result from magnetically-driven transitions from a KAM to a non-KAM system.

In numerical modeling of the experiments, a close fit to the MR extrema is only obtained by using a soft, as opposed to a hard-wall, potential. Within the dot this takes the form $V(x, y) = \frac{1}{2}m^*(\omega_{x,d}^2 x^2 + \omega_y^2 y^2)$ as shown for the single dot [17], while to model the constriction between two dots we use the saddle form $V(x, y) = \frac{1}{2}m^*(-\omega_{x,c}^2 x^2 + \omega_y^2 y^2) + E_c$. m^* is the effective mass of the electrons and E_c is the saddle-point energy. The anisotropy (elliptic shape) of the dots is taken into account by different values of the confinement parameters ω_y and $\omega_{x,d}$, with the potential having been adjusted to match what one obtains from fully self-consistent calculations [18]. Further details are described in Ref. [19]. The classical equation of motion for such an array is then solved by assuming ballistic transport, which is justified by the long mean free path of the 2DEG. In the presence of the magnetic field, the motion in the dot regions is harmonic with two hybrid frequencies [20]

$$\omega_\pm = \sqrt{\beta \pm \sqrt{\beta^2 - \omega_{x,d}^2 \omega_y^2}}, \qquad \beta = (\omega_{x,d}^2 + \omega_y^2 + \omega_c^2)/2, \tag{1}$$

where ω_c is the cyclotron frequency eB/m^*.

In the constrictions the motion is given by the superposition of a harmonic elliptic motion with frequency γ_+ and a nonperiodic motion along a hyperbola [where both $x(t)$ and $y(t)$ have $\cosh(\gamma_- t)$ and $\sinh(\gamma_- t)$ components]

$$\gamma_\pm = \sqrt{\mp\beta' + \sqrt{\beta'^2 + \omega_{x,c}^2 \omega_y^2}}, \qquad \beta' = (\omega_{x,c}^2 - \omega_y^2 - \omega_c^2)/2. \tag{2}$$

Trajectories are calculated on the Fermi surface by choosing starting angles and positions within the constriction or one of the dots. The presence of the constriction causes chaotic behavior which is modified by the magnetic field. To define a trajectory as either regular (periodic and quasiperiodic) or chaotic, the long-time behavior of the system must be studied. This is done by closing the array at its ends and studying the behavior for times as long as 10^{-6} s, several orders of magnitude longer than $1/\omega_\pm$. We determine that the peaks at ± 0.24, ± 0.54, and ± 0.70 T in Fig. 1(a) correspond, respectively, to trajectories with 2, 4, and 6 bounces at the "wall" of a dot. These field values can be expressed as even integer ratios of ω_+/ω_- [arrows in Fig. 1(a)]. Examples of the trajectories at these values, and the corresponding quantum probabilities, are shown in Fig. 1(b) (discussed below). The quantum calculation uses the same potential, with the transport computed by a recursive scattering matrix formulation based on the Lippman-Schwinger equation [21] and the conductance found from the Landauer equation [22].

To investigate states of the trajectories in the phase space [velocity (v_x, v_y), position (x, y)], Poincaré sections (PS) are computed at the center line of the dot array [$y = 0$, axes defined in Fig. 1(a)]. For a comparison of the classical phase-space dynamics with a quantum-mechanical (QM) analog, the Husimi distribution (HD) [15,23] is introduced. The electron wave function $\psi(x, y)$ is smoothed and transformed via a coherent state φ [15,23] centered at (x, y)

$$\varphi(x, k_x, y, k_y, x', y') = \left(\frac{1}{\pi\sigma^2}\right)^{1/4} \exp\left[-\frac{(x - x')^2 + (y - y')^2}{2\sigma^2} + ik_x(x' - x) + ik_y(y' - y)\right] \tag{3}$$

and, from this, the HD corresponding to a phase-space probability is created as

$$H(x, y, k_x, k_y) = \left| \int dx' dy' \psi(x', y') \varphi(x, k_x, y, k_y, x', y') \right|^2 \quad (4)$$

$k_x = m^* v_x/\hbar$, $k_y = m^* v_y/\hbar$. For comparison with the classical PS we project the cross section at $y = 0$ on top of the (x, v_x) plane

$$H^P(x, v_x) = \int dk_y H(x, y = 0, k_x, k_y). \quad (5)$$

Figure 2(a)–2(c) shows the PS-H^P representations for different values of ω_+/ω_- for $v_y > 0$. At $\omega_+/\omega_- = 1.6269$ ($B \approx 0.16$ T, low-field flank of the strongest MR peak), the PS in Fig. 2(a) consists of a large chaotic sea and two different types of periodically-arranged KAM islands, centered at $v_x = 0$ and marked as (1) and (2). Figure 3(a) shows a magnification from the two KAM islands presented in the PS-H^P representation of Fig. 2(a). At $v_x = 0$, the trajectories [Fig. 3(b), left] marked (1) and (2) correspond to the pure ω_+ [(1)] or the pure ω_- mode [(2)]. These orbits [Fig. 3(b), right] presumably correspond to the pointer states. The invariant curves around the center of a KAM island correspond to mixtures of the two modes. Each KAM island is surrounded by a "sticky" layer [7,10] emerging from trajectories that oscillate between a given dot and one of its constrictions for a long time before entering the sea of chaos. All trajectories with initial conditions in the sea of chaos are unstable and finally escape the dot array. The phase-space probability is distributed over the periodically arranged type-2 KAM islands and the neighboring chaotic regions. This is considered as evidence for phase-space tunneling involving the classically inaccessible KAM islands. An estimate of its contribution through the pointer states (corresponding to the orbits within a KAM island) can be obtained by using projection to decompose the wave function of the open dot array, dot by dot, in terms of eigenstates of the corresponding closed single dot [12,18]. For $\omega_+/\omega_- = 1.6269$, we find that the pointer state makes the dominant contribution, 46% when averaged over the array, much larger than any other individual state.

At $\omega_+/\omega_- = 2.0000$ ($B \approx 0.24$ T) the classical phase space in the PS-H^P representation is characterized by large regular regions with periodic and backscattered orbits embedded in a sea of chaos [Fig. 2(b)]. At this integer ratio, the regular regions are particularly large since the backscattered orbits exist and *many* stable periodic orbits fit into the dot region without penetrating the neighboring constrictions. Much of the sea of chaos has therefore been "drained" at this resonant condition. Since no quasiperiodic orbits exist, the system is non-KAM-like, but a slight deviation from resonance will restore the KAM-like behavior. As this occurs, the periodic orbits will have become

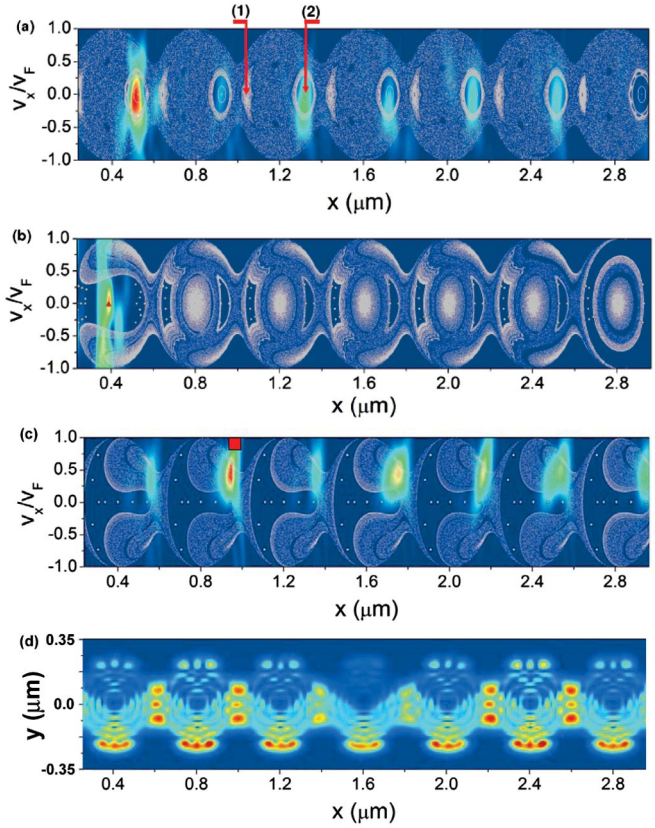

FIG. 2 (color). PS-H^P representations for different ratios of ω_+/ω_-: white dots represent the PS, color plots the H^P (red: high, blue: low QM phase-space probability). (a) $\omega_+/\omega_- = 1.6269$. The PS shows two types of KAM islands symbolized by (1) and (2) and a "sticky layer" (light gray) around them. The type-2 KAM islands in each dot have highest phase-space probability. (b) $\omega_+/\omega_- = 2.0000$. The large white dots, in the regions where the chaotic sea has been drained, correspond to different periodic orbits. The red triangle (first dot, highest probability) represents a backscattered orbit [same initial condition as in Fig. 1(b) at $\omega_+/\omega_- = 2.0000$]. (c) $\omega_+/\omega_- = 3.0000$. Large white dots: as in (b). The phase-space probability (for $v_y > 0$) is concentrated at the left transition between dot and constriction (symmetric with respect to the middle of the constriction if $v_y < 0$ data are included). The red rectangle indicates the size of $\hbar$, i.e., the QM uncertainty. (d) Probability density for $\omega_+/\omega_- = 3.0000$ (red: highest, blue: lowest probability).

quasiperiodic, resembling the closed periodic orbits but rotating at a rate $\Delta\omega = |\varepsilon|\omega$ where $\omega_+/\omega_- = n + \varepsilon$, $\varepsilon \ll 1$. In addition, the orbit curvature changes with magnetic field, causing a large number of orbits to penetrate the constrictions and leading to chaotic behavior [Figs. 2(a) and 3(a)]. The phase-space probability at $\omega_+/\omega_- = 2.0000$ is concentrated in the first dot with the highest density where classically backscattered trajectory cause points in the PS (e.g., red triangle). Because of the soft potential, the backscattered trajectory is strongly insensitive to its starting conditions, reflecting its high stability in phase space and causing the large resistance peak which is

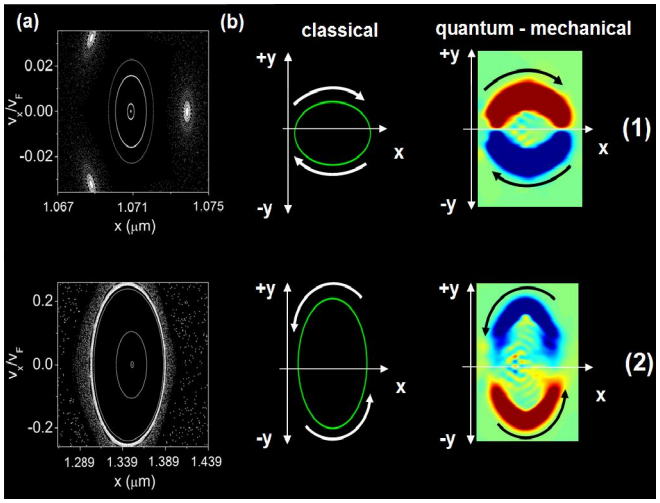

FIG. 3 (color online). Phase space of the 7-dot array for $\omega_+/\omega_- = 1.6269$ ($B \approx 0.16$ T). (a) Magnification of the two types of KAM islands in a two-dimensional (v_x, x) PS symbolized by (1) and (2) and a "sticky layer" (light gray) around them. $v_F = 2.1 \times 10^5$ m/s. (b) Left panel: trajectories at the center of the two KAM islands attributed to the pure ω_+ (1) and pure ω_- (2) mode, showing two different circulations. Right panel: probability current density (red: current flow to the right, blue: current flow to the left).

qualitatively repeated (but attenuated) at 0.54 T ($\omega_+/\omega_- = 4$) and 0.70 T ($\omega_+/\omega_- = 6$). A comparison of the classical orbits with their QM counterparts is shown in Fig. 1(b) for the three peaks of Fig. 1(a).

MR minima are found to be related to odd integer values of ω_+/ω_-. At $B \approx 0.43$ T, $\omega_+/\omega_- = 3$, skipping orbits form that are commensurate with the periodicity of the array [Fig. 2(d)]. These orbits enhance the transmission and dominate transport. Also at this resonance, the sea of chaos has been drained and the phase-space probability is now concentrated at the constrictions [Fig. 2(c)]. The corresponding probability density, which closely matches the skipping orbits, is shown in Fig. 2(d).

At noninteger but rational ratios such as 4/3 or 3/2, no significant structure is seen in the experimental MR. For these ratios, the classical phase space shows negligible draining of the sea of chaos and the QM calculations show little or no structure in the MR.

We may summarize these results in terms of the control of transport resulting from the influence of the magnetic field on the mixed phase space. The ratios ω_+/ω_-, which characterize the dynamics of a mixed phase space, are found to be essential also for the transport in the electron billiards. The MR maxima and minima indicate the formation of a non-KAM system, with even and odd ratios, respectively, of the characteristic frequencies. The corresponding PS are characterized by a mixed phase space with a reduced chaotic sea. Transmitted skipping orbits determine the transport for odd ratios of these frequencies, while for even ratios backscattered orbits are dominant. In the flanks of the MR peaks, in contrast, a mixed phase space consisting of large chaotic regions and KAM islands dominates. The orbits within the KAM islands that do not penetrate the constrictions presumably are connected to the pointer states, while the backscattered orbits and the transmitted skipping orbits arise from hybridization between the dot states and the environment states. All of this contributes to a fundamental understanding of the complicated landscape of interactions in open electron billiards.

This work was partly supported by FWF-Austria, Project no. 15513.

[1] *Quantum Theory and Measurement*, edited by J. A. Wheeler and W. H. Zurek (Princeton University Press, Princeton, NJ, 1983).
[2] E.g., K. Nakamura and T. Harayama, *Quantum Chaos and Quantum Dots* (Oxford University Press, New York, 2004).
[3] M. C. Gutzwiller, *Chaos in Classical and Quantum Mechanics* (Springer, New York, 1990).
[4] L. Pastur *et al.*, Phys. Rev. Lett. **93**, 063902 (2004); Y.-C. Lai *et al.*, Phys. Rev. Lett. **94**, 214101 (2005).
[5] R. Ketzmerick, Phys. Rev. B **54**, 10 841 (1996).
[6] E.g., H. W. Broer, Bull. Am. Math. Soc. **41**, 507 (2004).
[7] *Weak Chaos and Quasi-Regular Patterns*, edited by G. M. Zaslavsky *et al.* (Cambridge University Press, Cambridge, England, 1991).
[8] T. M. Fromhold *et al.*, Phys. Rev. Lett. **87**, 046803 (2001); Nature (London) **428**, 726 (2004).
[9] A. A. Chernikov *et al.*, Nature (London) **326**, 559 (1987).
[10] M. F. Shlesinger *et al.*, Nature (London) **363**, 31 (1993).
[11] W. H. Zurek, Rev. Mod. Phys. **75**, 715 (2003).
[12] D. K. Ferry, R. Akis, and J. P. Bird, Phys. Rev. Lett. **93**, 026803 (2004).
[13] D. K. Ferry, R. Akis, and J. P. Bird, J. Phys. Condens. Matter **17**, S1017 (2005).
[14] A. P. S. de Moura *et al.*, Phys. Rev. Lett. **88**, 236804 (2002).
[15] L. E. Reichl, *The Transition to Chaos* (Springer, New York, 2004).
[16] M. Elhassan *et al.*, Phys. Rev. B **70**, 205341 (2004).
[17] R. Brunner *et al.*, Physica (Amsterdam) **21E**, 491 (2004).
[18] R. Akis *et al.*, in *Electron Transport in Quantum Dots*, edited by J. P. Bird (Kluwer, Dordrecht, 2003).
[19] R. Brunner *et al.*, J. Comput. Electron. **6**, 93 (2007).
[20] A. Lorke, J. P. Kotthaus, and K. Ploog, Phys. Rev. Lett. **64**, 2559 (1990).
[21] R. Akis, D. K. Ferry, and J. P. Bird, Phys. Rev. B **54**, 17 705 (1996).
[22] R. Landauer, IBM J. Res. Develop. **1**, 223 (1957).
[23] K. Husimi, Proc. Phys. Math. Soc. Jpn. **22**, 246 (1940); B. Crespi, G. Perez, and S.-J. Chang, Phys. Rev. E **47**, 986 (1993).